J Mater Sci (2009) 44:1889–1893
DOI 10.1007/s10853-009-3279-0

Improved thermoelectric properties of La-doped $Bi_2Sr_2Co_2O_9$-layered misfit oxides

J. J. Shen · X. X. Liu · T. J. Zhu · X. B. Zhao

Received: 29 October 2008 / Accepted: 16 January 2009 / Published online: 11 February 2009

Abstract $Bi_2Sr_{2-x}La_xCo_2O_9$ ($x = 0$, 0.02, 0.04, and 0.08) polycrystalline-layered misfit oxides have been prepared by solid-state reactions. Electrical property measurements indicated that all the samples are *p*-type semiconductors. The electrical conductivity decreased and the Seebeck coefficient increased with increasing temperature. The thermal conductivities were very low, only 0.6–0.7 W m^{-1} K^{-1} at room temperature. La doping was effective in increasing the Seebeck coefficient, reducing the thermal conductivity, and hence improving the thermoelectric performance. A highest dimensionless figure of merit *ZT* of 0.147 was obtained for $Bi_2Sr_{1.96}La_{0.04}Co_2O_9$ sample at 737 K, about two times higher than that of the sample without La doping.

Introduction

Thermoelectric (TE) materials have been widely studied over the past decades due to the potential applications in power generation and electronic cooling. The performance of TE materials can be characterized by the dimensionless figure of merit $ZT = (\alpha^2\sigma/\kappa)T$, where α is the Seebeck coefficient, σ and κ are the electrical and thermal conductivities, respectively, and T is the absolute temperature. Nowadays, state-of-the-art TE materials are mainly semiconducting tellurides and antimonides such as Bi_2Te_3 [1], filled $CoSb_3$ [2], $Ag_nPb_mSb_nTe_{m+2n}$ [3], and so on. In spite of their high TE properties, certain shortcomings like low melting or decomposition temperatures and poor oxidation resistance are still needed to overcome [4]. Since the discovery of a large room temperature thermopower in $NaCo_2O_4$ [5], *p*-type-layered cobalt oxides, including γ-Na_xCoO_2 ($x \sim 0.7$) [6, 7], γ-Sr_xCoO_2 ($x \sim 0.35$) [8, 9], and $Ca_3Co_4O_9$ [10, 11] have attracted more and more attention. Because of their distinct advantages such as good thermal stability and low cost, these cobalt oxides have been considered as promising candidates for TE applications in recent years.

Recent studies have shown improved TE performance in PbSeTe/PbSe and Bi_2Te_3/Sb_2Te_3 superlattices [12, 13]. Theoretical calculations [14] indicated that an ultralow thermal conductivity could be obtained from the localization of lattice vibrations induced by the random stacking of two-dimensional crystalline sheets. Moreover, the Seebeck coefficient would increase along with the increased density of state of carriers arising from the anisotropy crystal structure. Therefore, $Bi_2Sr_2Co_2O_9$ (BSCO) misfit oxide material, which has not only the similar layered structure to the aforementioned cobalt oxides, but also natural superlattice substructures in the insulation layers, was expected to exhibit good TE properties. the single crystal BSCO whiskers were exposited having a *ZT* value of more than 1.1 at 1000 K [15], and a polycrystalline BSCO oxide has also been reported to a *ZT* value of about 0.19 at 973 K [16]. Researches about composition optimization of the BSCO oxide were processed, including composition adjustment and elemental doping. For example, a single crystal whiskers of Pb- and Ca-doped BSCO oxides have been referred exhibiting a relatively high power factor ($\alpha^2\sigma \sim 0.9$ mW m^{-1} K^{-2}) [17]. In addition, some more studies about BSCO, such as structure and thin film growth,

J. J. Shen · X. X. Liu · T. J. Zhu (✉) · X. B. Zhao (✉)
Department of Materials Science and Engineering, State Key Laboratory of Silicon Materials, Zhejiang University, No. 38 Zheda Road, Hangzhou 310027, China
e-mail: zhutj@zju.edu.cn

X. B. Zhao
e-mail: zhaoxb@zju.edu.cn

were also been conducted by Terasaki et al. [18] and Tsukada et al. [19].

To the best of our knowledge, there are few reports on TE properties of the rare earth-doped BSCO. In this study, La-doped $Bi_2Sr_{2-x}La_xCo_2O_9$ ($x = 0$, 0.02, 0.04, and 0.08) is prepared by conventional solid-state reactions, and the effects of La doping on the microstructure and TE properties are investigated.

Experimental

Stoichiometric ratio of Bi_2O_3, $SrCO_3$, La_2O_3, Co_3O_4 (>99%) was weighted and mixed according to the compositions of $Bi_2Sr_{2-x}La_xCo_2O_9$ with $x = 0$, 0.02, 0.04, and 0.08. The powder mixtures were fired at 1073 K for 10 h in air. After grinding, the reactants were pressed into pellets and sintered at 1113 K for 20 h in air. After that the samples were pulverized again by ball-milling and pelletized, and the final sintering was performed at 1163 K for 20 h in air. The relative densities of the four samples were ~85%.

Structure of the samples was investigated by X-ray diffraction (XRD) on a Rigaku D/MAX-2250P diffractometer using Cu Kα radiation (=1.5406 Å), and a FEI-siron field-emission scanning electron microscope (FESEM) was used to characterize the grain size and fracture surface morphology of the samples. The electrical conductivity and the Seebeck coefficient were simultaneously measured in air on a computer-assisted apparatus using a DC four-probe method and differential voltage/temperature technique, respectively [20]. The measurement errors of the electric properties are within 5%. In order to confirm the repeatability of the results, the samples were prepared and measured (both in vacuum and in air) several times, and the data showed an excellent consistency. Thermal conductivity was measured on a Netzsch® LFA 457 laser flash apparatus, and the measurement error is within 3%.

Results and discussion

Figure 1 is the XRD patterns for the $Bi_2Sr_{2-x}La_xCo_2O_9$ ($x = 0$, 0.02, 0.04, and 0.08) samples. The results show an excellent consistency with that reported by Kajitani et al. [21]. The strong (00*l*) diffraction peaks can be observed for all the samples due to the layered structure of the cobalt oxides. There are no obvious impurity phases and no notable diffraction peak shifts caused by the La doping due to the similar ionic radius between La^{3+} (1.15 Å) and Sr^{2+} (1.13 Å).

Figure 2 gives the SEM image of fracture surface of the undoped BSCO sample. The polyhedral sheet-like grains

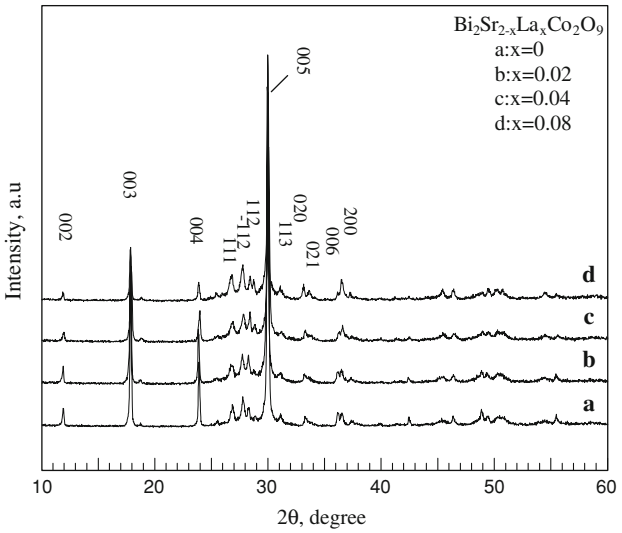

Fig. 1 XRD spectra of the $Bi_2Sr_{2-x}La_xCo_2O_9$ ($x = 0$, 0.02, 0.04, and 0.08) samples

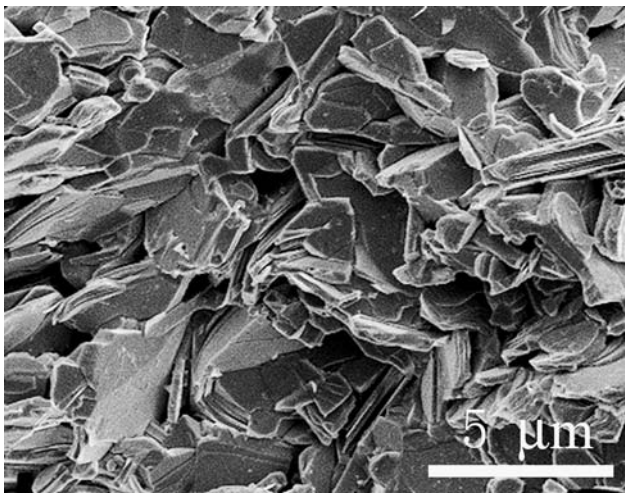

Fig. 2 SEM image of the sintered BSCO

show clearly the anisotropic growth of BSCO crystallites resulting from the layered structure of the oxides. Other $Bi_2Sr_{2-x}La_xCo_2O_9$ ($x = 0$, 0.02, 0.04, and 0.08) samples also exhibited the similar microstructures.

The temperature dependence of electrical conductivity for the $Bi_2Sr_{2-x}La_xCo_2O_9$ samples is shown in Fig. 3. The electrical conductivities of all the samples show a metal-like behavior ($d\sigma/dT < 0$) in the whole investigated temperature range. The σ decreases with increasing content of La, which could be attributed to the increasing impurity scattering and a difference in chemical valence between Sr^{2+} and La^{3+}. In order to keep the electro-neutrality condition in La-doped BSCO, the valence change of Co from Co^{4+} to Co^{3+} must have occurred, which makes the samples to have different average Co valences [22]. Cheng et al. [23] have already observed this change by X-ray

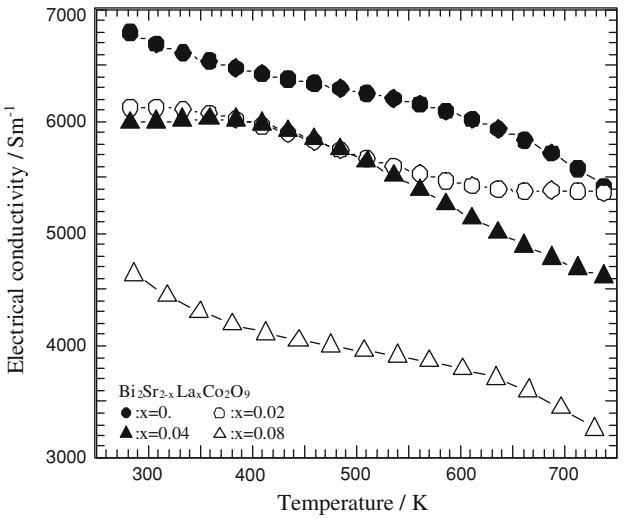

Fig. 3 Electrical conductivity as a function of temperature for $Bi_2Sr_{2-x}La_xCo_2O_9$ with $x = 0$, 0.02, 0.04, and 0.08

photoelectric spectrum. The Co–O layers in BSCO are the main bodies to conduct the electricity, and the carrier concentration will decrease with decreasing average Co valence [15]. Therefore, BSCO (Co^{4+}) without doping has the best electrical conductivity compared to the La-doped samples.

Figure 4 shows the temperature dependence of Seebeck coefficient α. The positive Seebeck coefficients indicate the *p*-type conduction in these samples. The α increases with increasing temperature, different from the result of Funahashi and Shikano [15], i.e., α decreases when $T < 673$ K. The Seebeck coefficient depends on band structure and scattering mechanisms. In general, the electrical conductivity of a conventional TE semiconductor

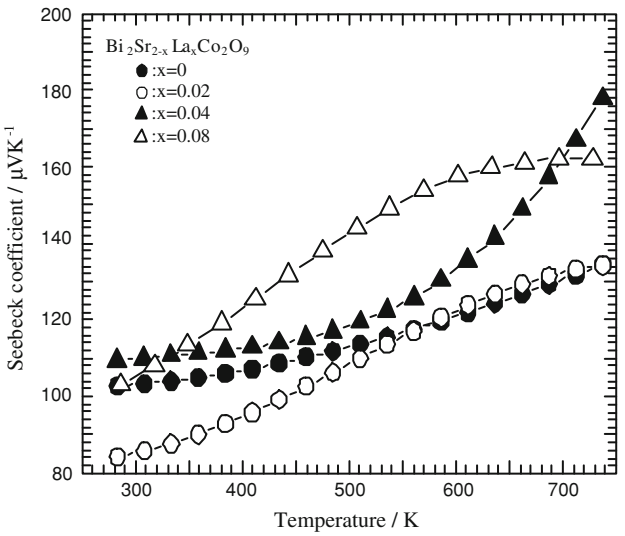

Fig. 4 Seebeck coefficient as a function of temperature for $Bi_2Sr_{2-x}La_xCo_2O_9$ with $x = 0$, 0.02, 0.04, and 0.08

decreases with increasing temperature before the intrinsic conduction, whereas the Seebeck coefficient increases with temperature due to the increased carrier scattering [24]. On the other hand, in this study, the substitution of La^{3+} for Sr^{2+} reduces negative charges in the lattice, which must be compensated either by reduction of holes. Thus, the concentrations of holes in the La-doped samples are smaller than that in the sample without doping, implying a higher Fermi energy. As a result, the samples with $x = 0.04$ and 0.08 have the higher Seebeck coefficients, and the former exhibits a maximum value of 180 μV K^{-1} at 750 K.

The charge carriers in *p*-type semiconductors are mobile holes. If holes are small polarons, the $\alpha - 1/T$ dependence can be expressed as [25, 26]:

$$\alpha - \alpha_0 \approx -\frac{k_B}{e}\ln\left(\frac{1-p}{p}\right) \approx \frac{E_g}{2eT}, \quad (1)$$

where k_B, p, e, and E_g are the Boltzmann constant, the hole concentration, the electronic charge, and the energy gap, respectively. And the electrical conductivity can be expressed as:

$$\sigma = pe\mu_P \sim T^{-1}\exp\left(\frac{-E_a}{k_B T}\right), \quad (2)$$

where μ_p is the mobility of holes and E_a is the activation energy.

The $1/T$ dependences of α and ln (T) of the BSCO samples are plotted in Fig. 5. It is clear that the small polaron conduction mechanism is applicable to all the samples below 450 K as the curves are almost linear. When the temperature further increases, the curves deviate from the linear trends, suggesting different conduction mechanisms at high temperatures. The results are similar to those of $La_{1-x}Sr_xCoO_3$ oxides [27]. With the increasing content of La, the slopes of both the $\alpha - 1/T$ and the ln (σT) $- 1/T$ curves change, indicating an alteration in the band structure. The calculated E_g below 450 K are 0.012, 0.030, 0.010, and 0.045 eV for the samples $x = 0$, 0.02, 0.04, and 0.08, respectively, comparable to the previous result by Terasaki et al. [28].

As shown in Fig. 6a, the thermal conductivity κ of $Bi_2Sr_{2-x}La_xCo_2O_9$ with $x = 0$, 0.02, 0.04, and 0.08 is plotted as a function of temperature. The κ exhibits a weak temperature dependence (i.e., around 0.7 W m^{-1} K^{-1}) in the tested temperature range, and shows a slight decrease after the La doping due to the increased phonon scattering by point defects. These values are much lower than those of other TE oxides, such as $Ca_3Co_4O_9$ [29]. As mentioned above, BSCO oxide has the special layered crystallographic structure, in which conducting and insulating layers are alternately piled, enhancing the phonon scattering at the interface [15]. In addition, the insulating layers own a natural superlattice structure in which Bi–O and Sr–O layers

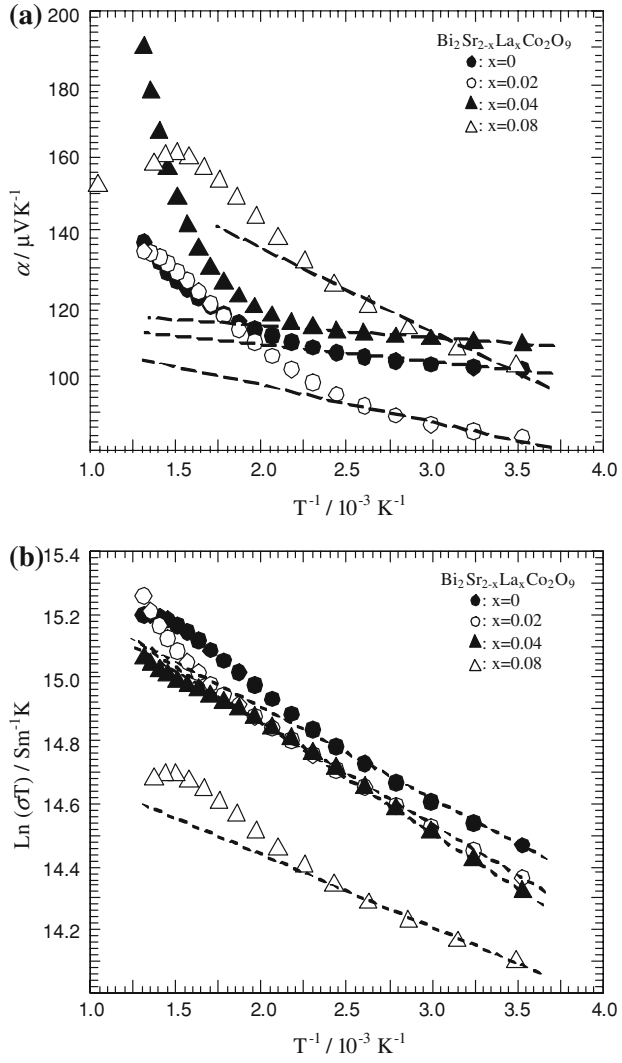

Fig. 5 Plots of α (**a**) and ln (σT) (**b**) versus $1/T$ for $Bi_2Sr_{2-x}La_xCo_2O_9$ with $x = 0$, 0.02, 0.04, and 0.08. The *dashed lines* are the fitting lines

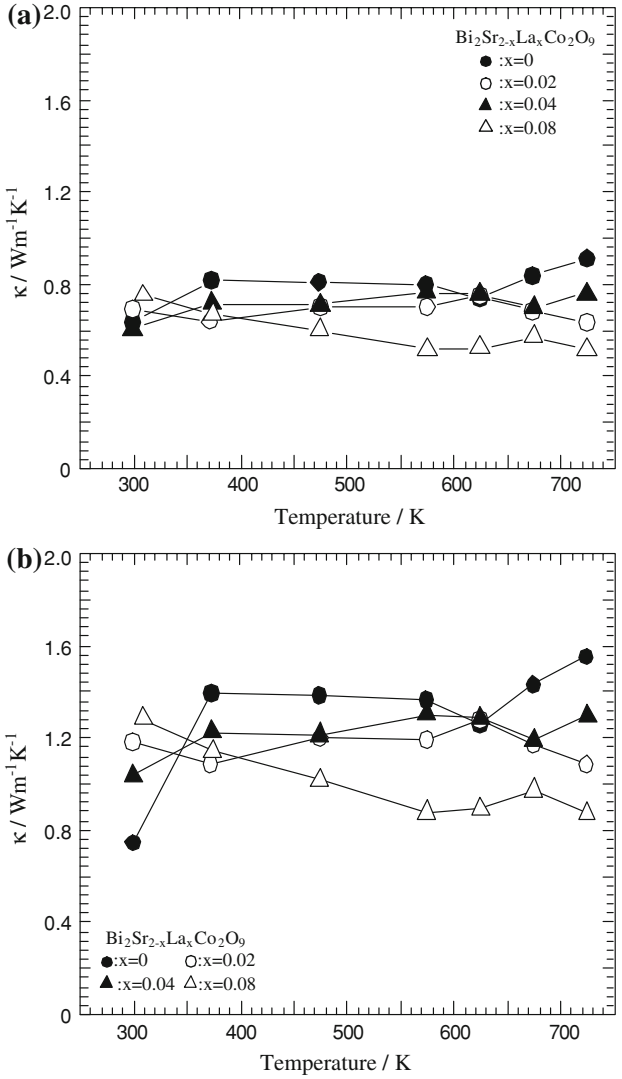

Fig. 6 **a** Temperature dependence of thermal conductivity for $Bi_2Sr_{2-x}La_xCo_2O_9$ with $x = 0$, 0.02, 0.04, and 0.08. **b** Temperature dependence of corrected thermal conductivity for $Bi_2Sr_{2-x}La_xCo_2O_9$ with $x = 0$, 0.02, 0.04, and 0.08

alternate with a period smaller than the mean-free path of phonons, which results in a phonon localization-like behavior and hence a lower κ value [29, 30].

Moreover, as the relative densities of the samples are ~85%, these samples have high porosities. In order to calibrate the thermal conductivity, the following Maxwell–Eucken equation was used,

$$\kappa = \kappa_0 \frac{1-p}{1+\beta p},$$

where p is the porosity, κ_0 the bulk conductivity, and β the constant number determined by the conditions of the pores (β is between 1.0 and 3.0 when the shape of the pores is almost the spherical style) [31]. Taking the porosity as 15% and the constant β as 3.0, the values of calculated κ_0 for the total four samples were still lower than other traditional ceramic oxides (around 1.2 W m^{-1} K^{-1}). The results are shown in Fig. 6b. However, as the porosity would also influence the electric properties of the bulk materials, here we should use the original value of the thermal conductivities to calculate to ZT value.

The dimensionless figure of merit ZT is calculated and presented in Fig. 7. The ZT value increases with increasing temperature. La doping improves the TE performance of BSCO oxide. Because of the relatively lower thermal conductivity and the higher Seebeck coefficient, $Bi_2Sr_{1.96}La_{0.04}Co_2O_9$ exhibits the highest ZT value of 0.147 at 737 K, which is nearly two times higher than that of the undoped sample and comparable to the ZT value of polycrystalline Pb-doped BSCO materials [32].

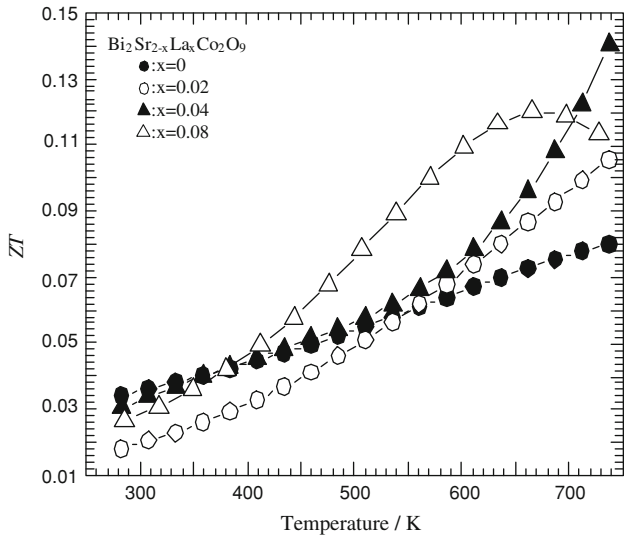

Fig. 7 Temperature dependence of figure of merit *ZT* for $Bi_2Sr_{2-x}La_xCo_2O_9$ with $x = 0$, 0.02, 0.04, and 0.08

Conclusions

Polycrystalline $Bi_2Sr_{2-x}La_xCo_2O_9$ ($x = 0$, 0.02, 0.04, and 0.08)-layered misfit oxides have been prepared by conventional solid-state reactions. All the samples are *p*-type semiconductors. The layered structure with natural superlattice of the misfit oxide leads to an ultralow thermal conductivity. The La doping increases the Seebeck coefficient, decreases the thermal conductivity, and hence improves the TE performance of this oxide effectively. The highest *ZT* value is about 0.147 at 737 K for $Bi_2Sr_{1.96}La_{0.04}Co_2O_9$, comparable to that of promising layered cobalt oxides $Ca_3Co_4O_9$.

Acknowledgements The study was supported by National "973" Program (2007CB607502), the National "863" Hi-tech Program of China (2007AA03Z234), and the Natural Science Foundation of China (50731006 and 50601022).

References

1. Zhao XB, Ji XH, Zhang YH, Zhu TJ, Tu JP, Zhang XB (2005) Appl Phys Lett 86:062111
2. Shi X, Zhang W, Chen LD, Yang J (2005) Phys Rev Lett 95:185503
3. Hsu KF, Loo S, Guo F, Chen W, Dyck JS, Uher C, Hogan T, Polychroniadis EK, Kanatzidis MG (2004) Science 303:818
4. Androulakis J, Migiakis P, Giapintzakis J (2004) Appl Phys Lett 84:1099
5. Terasaki I, Sasago Y, Uchinokura K (1997) Phys Rev B 56:R12685
6. Chang WJ, Hsieh CC, Chung TY, Hsu SY, Wu KH, Uen TM (2007) Appl Phys Lett 90:061917
7. Wang Y, Rogado NS, Cava RJ, Ong NP (2003) Nature 423:425
8. Ishikawa R, Ono Y, Miyazaki Y, Kajitani T (2002) Jpn J Appl Phys Part 2 41:L337
9. Sugiura K, Ohta H, Nomura K, Hirano M, Hosono H, Koumoto K (2006) Appl Phys Lett 88:082109
10. Masset AC, Michel C, Maignan A, Hervieu M, Toulemonde O, Studer F, Raveau B, Hejtmanek J (2000) Phys Rev B 62:166
11. Shikano M, Funahashi R (2003) Appl Phys Lett 82:1851
12. Harman TC, Walsh MP, LaForge BE, Turner GW (2005) J Electron Mater 34:L19
13. Venkatasubramanian R, Siivola E, Colpitts T, O'Quinn B (2001) Nature 413:597
14. Landry ES, Hussein MI, McGaughey AJH (2008) Phys Rev B 77:184302
15. Funahashi R, Shikano M (2002) Appl Phys Lett 81:1459
16. Funahashi R, Matsubara I, Sodeoka S (2000) Appl Phys Lett 76:2385
17. Funahashi R, Matsubara I (2007) Appl Phys Lett 79:362
18. Terasaki I, Tanaka H, Satake A, Okada S, Fujii T (2004) Phys Rev B 70:214106
19. Tsukada I, Nose M, Uchinokura K (1996) J Appl Phys 80:5691
20. Mi JL, Zhu TJ, Zhao XB (2007) J Appl Phys 101:054314
21. Kajitani T, Begum S, Yubuta K, Miyazaki Y, Igawa N (2007) The 26th international conference on thermoelectrics, Jeju Island, p 108
22. Mineshige A, Kobune M, Fujii S, Ogumi Z, Inaba M, Yao T, Kikuchi K (1999) J Solid State Chem 142:374
23. Li ZH, Cheng G, Jian P, Liu PS (2007) J Rare Earth 25:301
24. Cusack N, Kendall P (1958) Proc Phys Soc Lond 72:898
25. Senaris-Rodriguez MA, Goodenough JB (1995) J Solid State Chem 116:224
26. Nagao Y, Terasaki I (2007) Phys Rev B 76:144203
27. Zhou AJ, Zhu TJ, Zhao XB, Chen HY, Müller E (2008) J Alloys Compd 449:105
28. Xu GJ, Funahashi R, Shikano M, Matsubara I, Zhou YQ (2002) Appl Phys Lett 80:3760
29. Venkatasubramanian R (2000) Phys Rev B 61:3091
30. Majumdar A (2004) Science 303:777
31. Adachi J, Kurosaki K, Uno M, Yamanaka S (2007) J Alloys Compd 432:7
32. Xu GJ, Funahashi R, Shikano M, Matsubara IJ (2002) J Appl Phys 91:4344